

## Measurement of an Anisotropic Energy Gap in Single Plane $\text{Bi}_2\text{Sr}_{2-x}\text{La}_x\text{CuO}_{6+\delta}$

J. M. Harris,<sup>1</sup> P. J. White,<sup>1</sup> Z.-X. Shen,<sup>1</sup> H. Ikeda,<sup>2</sup> R. Yoshizaki,<sup>2</sup> H. Eisaki,<sup>3</sup> S. Uchida,<sup>3</sup>  
W. D. Si,<sup>4</sup> J. W. Xiong,<sup>4</sup> Z.-X. Zhao,<sup>4</sup> and D. S. Dessau<sup>5</sup>

<sup>1</sup>*Department of Applied Physics and Stanford Synchrotron Radiation Laboratory, Stanford University, Stanford, California 94305*

<sup>2</sup>*Institute of Applied Physics and Cryogenics Center, University of Tsukuba, Tsukuba, Ibaraki 305, Japan*

<sup>3</sup>*Department of Superconductivity, The University of Tokyo, Yayoi 2-11-16, Bunkyo-ku, Tokyo 133, Japan*

<sup>4</sup>*National Laboratory for Superconductivity, Institute of Physics, Chinese Academy of Sciences, Beijing 100080, China*

<sup>5</sup>*Department of Physics, University of Colorado, Boulder, Colorado 80309-0390*

(Received 4 March 1997)

We report angle-resolved photoemission spectra both above and below  $T_c$  in the single-plane cuprate superconductor  $\text{Bi}_2\text{Sr}_{2-x}\text{La}_x\text{CuO}_{6+\delta}$ . The superconducting state measurements show a highly anisotropic excitation gap with a maximum magnitude smaller than that of the bilayer compound  $\text{Bi}_2\text{Sr}_2\text{CaCu}_2\text{O}_8$  by a factor of 3. For a range of doping, the gap persists well above  $T_c$ , behavior previously associated with underdoped bilayer cuprates. The anisotropy and magnitude of the normal-state gap are very similar to the superconducting state gap, indicating that the two gaps may have a common origin in a pairing interaction. [S0031-9007(97)03519-9]

PACS numbers: 74.72.Hs, 71.18.+y, 74.25.Jb, 79.60.Bm

A central issue in the physics of high- $T_c$  superconductivity is the role of coupling between the two-dimensional copper-oxygen planes in producing superconductivity. The  $T_c$  of these materials tends to increase with the number of layers per unit cell. It is currently an open question whether the superconducting state order parameter symmetry will be the same in one-layer and the more strongly coupled two-layer compounds. Angle-resolved photoemission spectroscopy (ARPES) has the potential to resolve this issue since it is able to measure directly the anisotropy of the superconducting state gap (the magnitude of the order parameter). In the two-plane material  $\text{Bi}_2\text{Sr}_2\text{CaCu}_2\text{O}_{8+\delta}$  (Bi2212), the gap was found by ARPES to be highly anisotropic and consistent with a  $d_{x^2-y^2}$  order parameter [1,2]. We report measurements of the one-plane material Bi2201 that show a similarly large anisotropy with a smaller overall gap magnitude.

In underdoped Bi2212, ARPES measurements have shown that the anisotropic gap persists well above  $T_c$  [3,4], consistent with many other experiments that have shown a pseudogap or spin gap in the normal state of cuprate superconductors [5]. Current evidence for the normal-state gap in one-plane materials is much weaker than in two-plane materials, and its existence is controversial [6]. Our results show a clear normal-state gap up to high temperatures in optimally doped and underdoped Bi2201, but not in overdoped Bi2201.

Single crystal samples of  $\text{Bi}_{2+x}\text{Sr}_{2-(x+y)}\text{La}_y\text{CuO}_{6+\delta}$  were grown using a floating zone method, and for comparison by a self-flux method. X-ray scattering confirms that the crystals are single-phase Bi2201, and electron-probe microanalysis was used to measure the atomic ratios of the cations. Substitution of trivalent La or Bi for divalent Sr reduces the hole concentration in the  $\text{CuO}_2$  planes. The effect of La doping goes beyond changing the carrier density [7], however, and raises the maximum  $T_c$  from 10 to 30 K.

A roughly parabolic dependence of  $T_c$  on  $(x + y)$  has been observed [8]. Our optimally doped crystals ( $T_c = 29$  K) come from substituting  $\text{La} = 0.35$  for Sr. With no La substitution, Bi/Sr ratios of 2.3/1.7 and 2.1/1.9 give the underdoped samples with  $T_c < 4$  K and the overdoped samples with  $T_c = 8$  K, respectively. The transition temperatures were taken as the zero resistance values and confirmed by SQUID magnetization measurements. The transition widths are less than 2 K. The resistivity curves give linear- $T$  behavior for the optimally doped samples [8], positive curvature for the overdoped samples typical of other overdoped cuprates, and linear- $T$  dependence for the underdoped samples with an upturn at low  $T$ .

The angle-resolved photoemission measurements were carried out in two different ARPES systems for all types of samples, giving consistent results. In one case the photon source is unpolarized with 21.2 eV photons and a total resolution of 20 meV FWHM, while in the other case 22.4 eV linearly polarized photons were used with a resolution of 35 meV FWHM. The spectra in the figures came from the second (35 meV) system, while data in Fig. 3, shown below, came from both systems. The analyzer acceptance angle was  $\pm 1^\circ$ , corresponding to a  $k$ -space window of radius  $0.045\pi/a$  or  $0.037 \text{ \AA}^{-1}$ . Base pressures of the vacuum systems were  $4 \times 10^{-11}$  torr, and Fermi energies were determined from a reference Au film. Low energy electron diffraction (LEED) measurements confirm the quality of the UHV-cleaved surfaces and show a Bi-O plane superstructure that is well known in Bi-based cuprates.

Fermi surface (FS) crossings were determined from at least 5  $k$ -space cuts in one octant of each Bi2201 sample. Two cuts along high symmetry lines are plotted for three samples with different doping levels in Fig. 1. The data consist of energy distribution curves (EDCs) taken in the *normal state* at fixed  $k$ , determined by the angles between

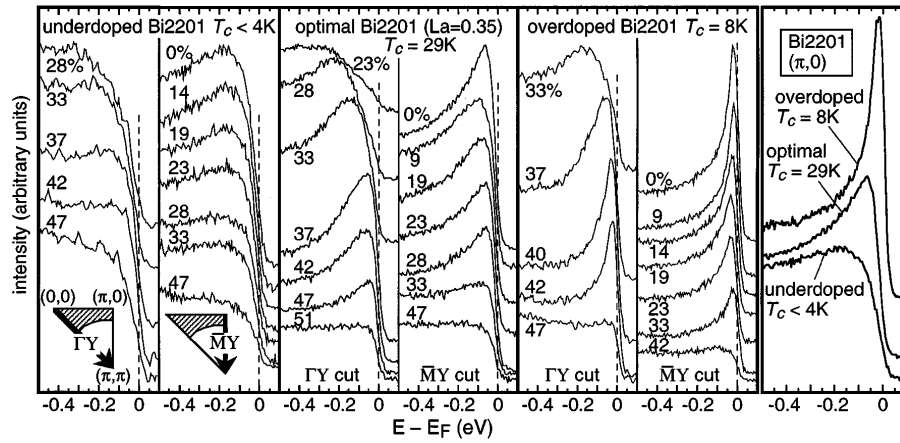


FIG. 1. Normal-state ARPES spectra for underdoped ( $T_c < 4$  K), optimally doped ( $T_c = 29$  K), and overdoped ( $T_c = 8$  K) Bi2201, measured at  $T = 100, 60,$  and  $60$  K, respectively. The left panels for each doping show spectra along the  $\Gamma Y$   $k$ -space cut while the right panels show the  $\bar{M}Y$  cut. The rightmost panel shows the strong change in linewidth with doping at  $(\pi, 0)$ .

the sample normal and electron analyzer. A number of nearly equivalent criteria can be applied to finding the positions of FS crossings along  $k$ -space cuts, such as identifying the point where the peak intensity decreases by one-half in going from occupied to unoccupied states, or where the leading edge midpoint of the spectral weight comes closest to  $E_F$ . The latter (leading edge midpoint position) is useful because it is also a measure of a gap in the excitation spectrum when it fails to reach  $E_F$  [1]. The measured Fermi surface in our samples is similar to previous work on overdoped Bi2201 [9] showing a large hole pocket centered on  $(\pi, \pi)$ . We find that over a wide range of doping, there is little change in the FS and no indication of a FS topology change.

The cuts in Fig. 1 are along  $(0,0)$  to  $(\pi, \pi)$  [ $\Gamma Y$  cut] and  $(\pi, 0)$  to  $(\pi, \pi)$  [ $\bar{M}Y$  cut]. The  $\Gamma Y$  cuts (left panels) show the largest energy dispersion and clear FS crossings in the vicinity of  $(0.4\pi, 0.4\pi)$ . (We plot  $\Gamma Y$  instead of  $\Gamma X$  because there is less complication from superstructure effects.) The  $\bar{M}Y$  cuts (right panels) show much less dispersion, but FS crossings can still be seen near  $(\pi, 0.25\pi)$ . The most striking change with doping occurs in the line shape. As the hole doping increases, the line shape becomes much narrower, indicating that the imaginary part of the excitation's self-energy has dramatically decreased. Only the overdoped Bi2201 sample approaches Fermi-liquid-like behavior with well-defined quasiparticle excitations. The linewidth at  $(\pi, 0)$  is especially sensitive to doping, as shown in the rightmost panel. The underdoped sample barely has a peak at all, while the overdoped sample has a large peak that is nearly resolution limited. Disorder may play a role in the trend of these normal-state spectra, assuming that Matthiessen's rule holds, since the residual resistivity increases from the overdoped to the underdoped crystals. The residual resistivity ratio [forming  $R(300\text{ K})/R(0\text{ K})$  by extrapolating to 0 K] is 3.7 for the overdoped case, 2.4 for optimal, and 2.0 for underdoped. However, the similarity to the trend of linewidth in Bi2212 suggests that doping is the primary cause of the linewidth

change. In Bi2212, the linewidths of underdoped samples are very broad, but sharp, resolution-limited peaks still appear below  $T_c$ , indicating impurity scattering is not dominant in these systems [4].

We next turn to the important issue of the superconducting state gap. As mentioned above, the shift in the leading edge midpoint may be used to characterize an excitation gap. In the overdoped case, no gap is observable within our resolution. This can be seen from the spectra on the FS taken from the  $\Gamma Y$  and  $\bar{M}Y$  cuts (Fig. 2). The leading edges of both overdoped spectra coincide. Since the BCS gap for  $T_c = 8$  K is only 1.5 meV, it is not surprising that the gap is too small to be seen within our error bars of  $\pm 2$  meV. In the optimally doped samples, however, we observe a clear and reproducible gap of  $10 \pm 2$  meV, in rough agreement with point contact tunneling measurements on ceramic samples of similar composition [10]. The gap is anisotropic, with a maximum on the  $\bar{M}Y$  cut [i.e., near  $(\pi, 0)$ ] and a minimum consistent with 0 on the  $\Gamma Y$  cut  $45^\circ$  away. Comparing these two extremes (Fig. 2) shows the shift in leading edge position quite clearly. Furthermore, we have reproduced the same gap value within error bars on 3 other samples. Interestingly, the gap persists into the normal state with no noticeable diminution. In the underdoped sample, the leading edges are not as sharp, but a reproducible gap of  $7 \pm 3$  meV maximum magnitude is still evident.

The measured Bi2201 superconducting state line shape differs from that of Bi2212 because it lacks the "peak and dip" feature. In Bi2212, the sharp peak is at  $\sim 40$  meV binding energy, followed by a dip that extends to  $\sim 90$  meV [11]. If the features scale in energy with the gap [12], then the factor of 3 decrease for Bi2201 would make them difficult to resolve. It is also possible that impurity scattering plays a role in obscuring any line shape change. Instead of a sharp peak and dip, our spectra show a moderate linewidth narrowing below  $T_c$  (Fig. 2).

To explore the gap anisotropy, we took a number of  $k$ -space cuts between the  $\Gamma Y$  and  $\bar{M}Y$  cuts of Fig. 1 on

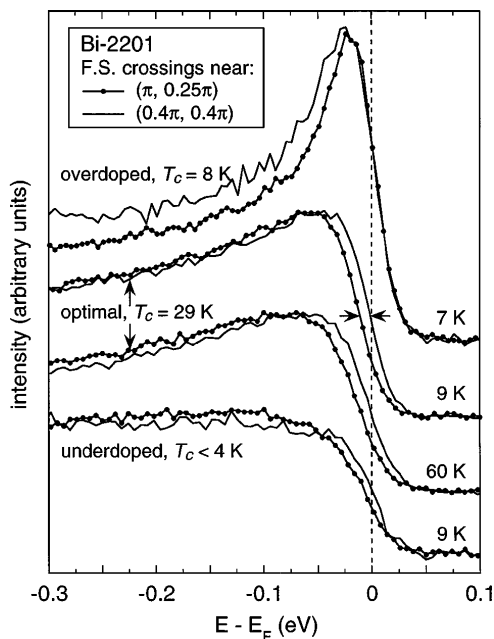


FIG. 2. ARPES spectra at FS crossings for the maximum [near  $(\pi, 0.25\pi)$ ] and minimum [near  $(0.4\pi, 0.4\pi)$ ] gaps for the crystals of Fig. 1. Shifts in the leading edge midpoints indicate an anisotropic gap, as in the  $10 \pm 2$  meV shift between the arrows for the  $T_c = 29$  K samples at  $T = 9$  K. The spectra are normalized to give the leading edges equal height in order to show the shifts between them.

the same samples. The leading edge shifts representing the excitation gap for two optimally doped Bi2201 samples are plotted vs  $0.5|\cos k_x a - \cos k_y a|$  both below and well above  $T_c$  in Fig. 3. On this plot, a  $d_{x^2-y^2}$  gap would be a straight line through the origin. The curves show considerable flattening near the origin compared to a pristine  $d$ -wave gap, suggestive of either the effect of interlayer tunneling matrix elements [13,14] or pair breaking due to impurities [15].

A central purpose of the present study was to determine whether the superconducting state gap anisotropy persists as the  $\text{CuO}_2$  planes are increasingly isolated from each other. Our observation of a strongly anisotropic gap in Bi2201 indicates that it does, since Bi2201 has a large separation between  $\text{CuO}_2$  planes ( $12.3 \text{ \AA}$  compared to  $3.3 \text{ \AA}$  for Bi2212), a huge  $c$ -axis resistivity ( $\rho_c = 30 \text{ \Omega cm}$  at 50 K [8]), and nonmetallic intervening Bi-O layers. A theoretical model that may be relevant to our findings is the interlayer tunneling (ILT) model [13], since it addresses the effect of interplanar coupling on the gap magnitude and anisotropy. In the ILT model, the *sign* of the order parameter is determined by the in-plane pairing kernel, which acts as a symmetry breaking field in the space of order parameter symmetries [14,16]. However, the anisotropy in *gap magnitude* is dominated by the effect of interlayer matrix elements [13,14] when  $T_c$  is high. Thus small  $s$ -wave or  $d$ -wave in-plane pairing kernels in the presence of strong interlayer coupling would give nearly identical results in ARPES gap magnitude measurements.

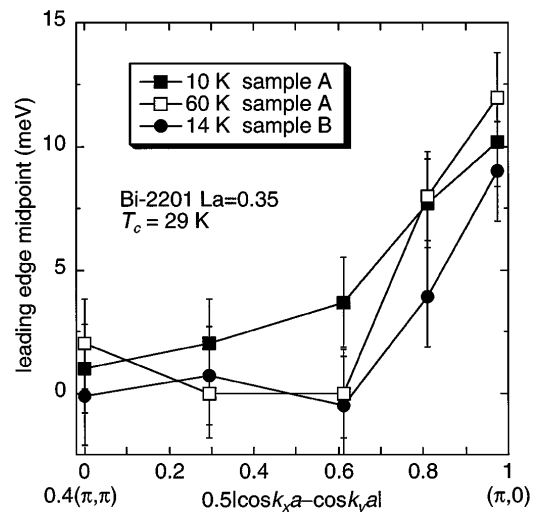


FIG. 3. Leading edge midpoint shifts from  $E_F$  for samples A and B, indicative of an anisotropic energy gap in the superconducting and normal states of optimally doped Bi2201. A  $d_{x^2-y^2}$  gap is a straight line intercepting the origin of the plot.

Weakening the interlayer coupling more clearly reveals the intrinsic single-plane gap. The highly anisotropic gap in Bi2201 is consistent with an underlying  $d_{x^2-y^2}$  symmetry, perhaps with some residual interlayer pair tunneling.

Our results mesh well with the tricrystal experiments of Tsuei *et al.* carried out on the single-plane cuprate Tl2201. The half-integer flux quanta observed in the superconducting state indicate a sign change in the order parameter [17]. Thus the intrinsic interaction in a single plane favors  $d$ -wave pairing, while the overall increase in gap magnitude from Bi2201 to Bi2212 by a factor of 3 may indicate that interlayer coupling enhances the gap [13,14,16]. Even in Bi2201 the gap magnitude greatly exceeds the BCS prediction of 4.4 meV for  $T_c = 29$  K (the leading edge midpoint shift tends to underestimate the gap).

It is important to consider whether disorder and impurities cause the gap to be smaller in Bi2201 than in Bi2212. The residual resistivity ratio (RRR) is 2.4 for optimally doped Bi2201, a rather low value that indicates substantial impurity scattering. However, some thin films of Dy-doped Bi2212 have even smaller RRRs, and they show no reduction in gap magnitude [4]. Thus the lower gap magnitude in Bi2201 is most likely intrinsic.

The measurements of a normal-state gap in Bi2201 (Figs. 2 and 3) show that the pseudogap can exist in a one-plane material. A pairing enhancement based on interlayer superexchange  $J_{\perp}$ , suggested for bilayer materials [6,18], will be absent in Bi2201 because of the large distance between  $\text{CuO}_2$  planes and the geometric frustration induced by the staggering of Cu sites along the  $c$  axis. As in the case of Bi2212 [3], the similarity in gap anisotropy and magnitude above and below  $T_c$  suggests that the two gaps are related and that pairing occurs well above  $T_c$ . Further evidence for this point of view has come from low

temperature gap measurements in Bi2212. The gap fails to decrease with  $T_c$  as  $T_c$  is decreased by underdoping [4]. The persistence of the gap in the underdoped Bi2201 sample shows the same anomalous pattern; the gap in underdoped samples represents a different energy scale from  $kT_c$ . Theoretical interpretations of separate energy scales for the gap and  $kT_c$  have included the idea that pairs form at relatively high temperatures but do not become phase coherent until  $T_c$  [19]. Microscopic theories based on spin-charge separation have separate pairings for spin and charge excitations [20], with spinon pairing occurring in general at a higher temperature than holon pairing.

The gap measurements on Bi2201 and Bi2212 as a function of doping show a striking contrast between the effect of lowering  $T_c$  by underdoping and lowering  $T_c$  by weakening the interplanar coupling. The gap (and thus the pairing strength) is relatively insensitive to underdoping but drops roughly proportionally to the maximum  $T_c$  in going from a bilayer to single layer material.

While no detailed theory exists for the line shape evolution with doping, the change from a narrow peak to a broad continuum with decreasing hole doping suggests non-Fermi-liquid behavior and a breakdown of the quasiparticle picture. Recently, it was proposed that the peak width is due to the strong coupling of electrons to collective excitations with  $\mathbf{q}$  peaked at  $(\pi, \pi)$  [21]. The width has also been attributed to the decay of the hole into a spinon and holon [22], with the hole lifetime decreasing on the underdoped side. The rightmost panel of Fig. 1 shows the line shape trend clearly and is insensitive to finite  $k$  resolution because the dispersion is small near  $(\pi, 0)$ .

In summary, ARPES measurements of the gap and electronic structure of the one-plane compound Bi2201 open a new window on the occurrence of superconductivity in a relatively low- $T_c$  member of the cuprate family. These observations constrain theories by showing that in a system with very weakly coupled planes, there is a strongly anisotropic superconducting gap and also a pseudogap above  $T_c$ .

We acknowledge helpful discussions with S. Chakravarty, S. Strong, S. Kivelson, P.W. Anderson, R.B. Laughlin, and P.A. Lee. SSRL is operated by the DOE Office of Basic Energy Sciences, Division of Chemical Sciences. The work at Stanford was supported by ONR Grant No. N00014-95-1-0760; the Division of Materials Science, DOE; and NSF Grant No. DMR 9311566. H.I.

and R. Y. acknowledge a Grant-in-Aid from the Ministry of Education, Science, Sports and Culture, Japan.

- 
- [1] Z.-X. Shen *et al.*, Phys. Rev. Lett. **70**, 1553 (1993).
  - [2] H. Ding *et al.*, Phys. Rev. B **54**, R9678 (1996).
  - [3] D.S. Marshall *et al.*, Phys. Rev. Lett. **76**, 4841 (1996); A.G. Loeser *et al.*, Science **273**, 325 (1996); H. Ding *et al.*, Nature (London) **382**, 51 (1996).
  - [4] J.M. Harris *et al.*, Phys. Rev. B **54**, R15665 (1996).
  - [5] For example, see N.P. Ong, Science **273**, 321 (1996); B. Batlogg and V.J. Emery, Nature (London) **382**, 20 (1996); B.G. Levi, Phys. Today **49**, No. 6, 19 (1996), and references therein.
  - [6] A.J. Millis and H. Monien, Phys. Rev. Lett. **70**, 2810 (1993).
  - [7] H. Nameki *et al.*, Physica (Amsterdam) **234C**, 255 (1994).
  - [8] R. Yoshizaki, H. Ikeda, L.-X. Chen, and M. Akimatsu, Physica (Amsterdam) **224C**, 121 (1994).
  - [9] D.M. King *et al.*, Phys. Rev. Lett. **73**, 3298 (1994).
  - [10] N. Hudáková *et al.*, Physica (Amsterdam) **218B**, 217 (1996).
  - [11] D.S. Dessau *et al.*, Phys. Rev. Lett. **66**, 2160 (1991).
  - [12] C.M. Varma and P.B. Littlewood, Phys. Rev. B **46**, 405 (1992).
  - [13] S. Chakravarty, A. Sudbø, P.W. Anderson, and S. Strong, Science **261**, 337 (1993).
  - [14] L. Yin, S. Chakravarty, and P.W. Anderson (to be published).
  - [15] L.S. Borkowski and P.J. Hirschfeld, Phys. Rev. B **49**, 15404 (1994).
  - [16] A. Sudbø and S.P. Strong, Phys. Rev. B **51**, 1338 (1995).
  - [17] C.C. Tsuei *et al.*, Science **271**, 329 (1996).
  - [18] M.U. Ubbens and P.A. Lee, Phys. Rev. B **50**, 438 (1994); B.L. Altshuler, L.B. Ioffe, and A.J. Millis, Phys. Rev. B **53**, 415 (1996).
  - [19] V.J. Emery and S. A. Kivelson, Nature (London) **374**, 434 (1995); S. Doniach and M. Inui, Phys. Rev. B **41**, 6668 (1990).
  - [20] P.W. Anderson and S.P. Strong, Chin. J. Phys. **34**, 159 (1996); P.W. Anderson, J. Phys. Condens. Matter **8**, 10083 (1996); X.-G. Wen and P.A. Lee, Phys. Rev. Lett. **76**, 503 (1996); V.J. Emery, S.A. Kivelson, and O. Zachar, Report No. cond-mat/9610094; H. Fukuyama, Physica (Amsterdam) **263C**, 35 (1996).
  - [21] Z.-X. Shen and J.R. Schrieffer, Phys. Rev. Lett. **78**, 1771 (1997).
  - [22] R.B. Laughlin, Report No. supr-con/9608005.